

ANALYSIS OF MECHANICAL AND CHEMICAL PELLET-CLAD INTERACTION DURING POWER RAMPS

W. VOGL, W. HERING, M. PEEHS
Kraftwerk Union AG, D-8520 Erlangen, Germany

J. LAVAKE

Combustion Engineering Inc., 1000 Prospect Hill Road, Windsor, Connecticut, 06095, U.S.A.

Summary

A research and development program is being conducted by KWU and C-E to investigate Pellet/Clad Interaction (PCI) in LWR fuel rods during power ramping. Out-of-pile iodine stress corrosion cracking studies, in-pile ramp experiments and hot cell chemical and metallographical post-irradiation examinations are being performed to study and evaluate both the power limitations and the basic mechanisms of PCI as well as practical methods to improve ramping performance.

Laboratory Iodine Stress Corrosion Cracking (I-SCC) results from both internally pressurized tube-type stress rupture tests and more sophisticated, constant load split ring tests show very clearly that a threshold for the iodine concentration must be exceeded and a certain strain rate or stress must be applied to produce cracks in a given time period. These results, when applied to actual ramp tests, help to explain the performance of over 80 ramped rodlets that were pre-irradiated in a commercial power plant for up to 2 cycles and then ramped in test reactors. Three types of ramp tests have been performed: (1) start-up tests which simulate the initial power ramp during the start-up after refuelling, (2) in-situ tests which represent a power increase during normal reactor operation, e.g. due to a control rod withdrawal, and (3) modified in-situ ramp tests performed with a slower ramp rate in the upper range of the ramp power.

Under these various conditions, the rodlets have been tested to powers of up to approximately 680 W/cm at rates of up to 100 W/cm min. Results show a correlation between time of defect and ramp terminal power which is comparable to the laboratory results on stress corrosion cracking. Post-irradiation examinations have shown mechanical interactions in the form of UO₂ pellet end dish closure and cladding ridges at the pellet interfaces

as observed in neutron radiography, metallography, and profilometry; these results are dependent on local rod power, pellet geometry, burnup and type of ramp test. Redistribution of fission products, as determined from gamma-scans, shows that a threshold power must be exceeded for migration of fission products to pellet interfaces and pellet cracks. Fission gas release measurements show a similar behaviour with expressed dependence on rod power.

Analytical evaluation of ramp test results are being performed using fuel performance evaluation codes. At present, KWU has evaluated ramp test results by the use of the computer Code CARO together with an empirical method called interference approach. This approach normalizes the average mechanical clad hoop strain during a ramp by taking into account the design parameters (e.g. initial gap size) and the power history of the fuel rod. The failure/non-failure intersection line in an interference versus burnup plot depends on burnup. This indicates that chemical effects are also important for the PCI behaviour besides mechanical effects.

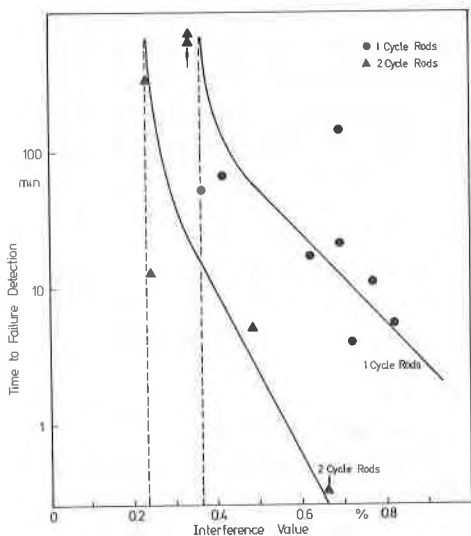


Figure 1
Ramp Peak Power as a Function of Burnup for PWR Fuel Rods (Pre-Pressurized UO_2 Fuel), Status Feb.79

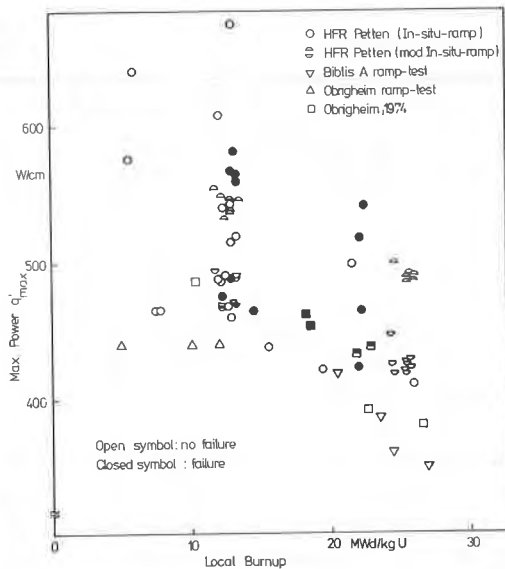


Figure 2
Petten Ramp Test Results, Time to Failure as a Function of the Interference Value (1 Cycle and 2 Cycle Rodlets)

1. Introduction

When a fuel rod in a nuclear power plant experiences a sudden increase in power above its steady-state-operation power level, the cladding is strained by the thermally expanding pellets. In addition, volatile fission products (VFP) are redistributed and released from the fuel to the cladding by the temperature increase of the fuel. This combined mechanical and chemical pellet-clad interaction, through a SCC mechanism, may lead to fuel rod failures in a power range where purely mechanical defects are not possible. Both KWU and C-E conduct research and development programs to investigate PCI and to improve fuel rod performance under ramp conditions /1 - 4/. This paper gives an up-to-date status of our investigations.

2. Experimental Results

2.1 In-File-Ramp Experiments

The first aim of the performed ramp experiments was to get the power limitations of pre-pressurized PWR standard fuel rods. The main experimental parameter was therefore the ramp power. The ramp rate was, when possible, fixed to 100 W/cm min, which represents a fast rate in operating power plants. In some experiments the ramp rate was lowered with the intent to overcome the defect threshold power of fast ramps. Fig.1 shows a plot of the ramp power versus burnup. The diagram includes data points from the Petten program and from the power reactor ramp tests in Obrigheim and Biblis /1/. In the latter case, only a few characteristic rods have been selected for the evaluation; the actual number of data points is several hundred. These ramp results indicate a defect threshold which decreases from approx. 480 W/cm at about 12 GWd/t(U) to approx. 420 W/cm at about 24 GW/t(U), below which no defects occur. It was possible to increase this threshold by approx. 70 W/cm by different rod designs, or by reducing the ramp rate (modified in-situ ramps). The time to failure continuously decreases as the ramp power is increased as shown by Fig.2, which shows the time to failure versus the interference value (see chapter 3).

Post irradiation examinations of the ramped rodlets have shown mechanical interactions in the form of UO₂ pellet end dish closure and cladding ridges at the pellet interfaces as observed in neutron radiography, metallography, and profilometry. These results are dependent on local rod power, pellet geometry, burnup and type of ramp test. Redistribution of fission products, as determined from gamma-scans /5/ (Fig.3), shows that a threshold power must be exceeded for migration of fission products to pellet interfaces and pellet cracks. Fission gas release measurements show a similar behaviour with expressed dependence on rod power (Fig.4). The failures

are always located at pellet interface positions and there does not seem to exist a relation between ridge height and the failure mechanism. The measurements of the grain growth induced by the ramp indicate that defects only occur if a distinct temperature level is exceeded. The features of the cladding cracks as shown from cross sections at defect positions are typical for SCC-cracks.

2.2 Out-of-Pile Experiments

Out-of-pile I-SCC tests have been performed using both the standard pressurized tube tests containing iodine and a more sensitive laboratory-type test using a sheet or split ring sample in a creep rupture-type apparatus with controlled iodine partial pressure. The laboratory test has provided a description of the I-SCC kinetics as shown in Fig.5 /6/. Here the incubation, failure progress, and propagation phases have been described. Furthermore, acoustical emission analyses showed most activity to occur within the first 2 or 3 minutes after iodine was introduced and the integrated activity increased with increasing iodine concentrations.

Tests were also run with iodine being introduced before, simultaneously with, or after the stress was applied. Fig.6 shows that if iodine is introduced up to approx. 1 hour before the stress is applied, the time to rupture is shorter than if the iodine and stress were applied simultaneously. However, it is also shown that if the iodine is introduced still earlier, then the time to failure increases again. Other experiments showed that the I-SCC-behaviour of freshly formed zirconium iodides was the same as that of gaseous iodine. Further tests have shown a dependence of time-to-failure on strain rate where a minimum failure strain and time-to failure occur at approx. 10^{-3} /hr strain rate.

3. Interference Approach

With this model /7/, the circumferentially averaged mechanical hoop strain in the clad during a ramp which is a function of the design parameters (e.g. initial gap size, prepressure etc.) and the power history of a fuel rod is calculated. The initial conditions just prior to ramping are calculated by the CARO Code. The clad hoop strain during the ramp is derived from the fuel/clad interference as determined by the different thermal expansions of the fuel and the cladding.

During pre-irradiation, reversible relocation of the fuel is assumed. This means that after gap closure the pellet fragments can be pushed back

without considerable reaction forces until the pellet relocation is offset. However, during the ramp itself the "residual" pellet relocation is treated as non-reversible. Furthermore, creep and relaxation effects in the fuel and in the clad are neglected at present. In Fig.7 all fast power ramps on pre-pressurized fuel rodlets from KWU/C-E are evaluated by plotting the interference values versus burnups. The failure/non-failure intersection line drawn through these preliminary results is valid for ramps starting from about 300 W/cm and having a ramp rate of approx. 100 W/cm min.

4. Discussion

The preceeding experimental results have given us an insight for describing PCI failures. Of prime importance is the fact that the PCI defect mechanism can only start after fresh release of SCC producing VFP's to the cladding. This is shown by our data, since the LHGR of iodine redistribution (approximately 350 W/cm) is markedly below the critical threshold power for PCI defects in the investigated burnup range. However, it should be realized that the failure range is not sharply defined, but is rather a failure probability band /1/. When all fuel rod and all experimental parameters are essentially the same, as in the Interramp experiments /8/, the failure range seems to be better defined.

Also of prime importance is the observation that, within the investigated range, the interference threshold decreases with increasing burnup. Since the interference value takes into account increased swelling with burnup, a possible explanation would be that at higher burnups the critical amount of VFP's is released at lower fuel temperature because of the higher amounts stored in the fuel. Of course, other burnup effects, such as a changing creep strength of the fuel would also influence the PCI behaviour.

Our observations have been condensed into a hypothesis describing the time dependence of mechanical and chemical components of PCI over the investigated ramp power region. This is described schematically in Fig.8, where the thermal feedback effect /2/ has been disregarded. At powers below the defect threshold (8a), the critical thresholds for neither stress nor VFP's are reached. At the defect threshold, 8b, we have the situation (see Fig.6) where the critical stress is reached before the critical VFP concentration, which is reached considerably after the end of the ramp. By ramping to within the defect region, 8c, the stress and VFP's markedly exceed their thresholds, resulting in a short time to failure.

Some experiments at low burnups, see Figs.1 and 7, indicate a non-failure area above the failure region. In this case, 8d, the fast relaxation of the hot fuel reduces the cladding stress before the critical threshold stress is reached. Such fast relaxation has been seen in Halden experiments by length measurements of fuel rods during high power ramps /9/.

The preceding hypothesis explains well our observations from these ramp tests. However, to understand more fully the PCI mechanism and to be able to improve fuel rod performance under ramp conditions, we need more data on the time dependence of the mechanical and chemical interaction between pellet and clad. Future experiments with instrumentation for internal fuel rod pressure measurements as well as fuel rod and fuel column length measurements during ramping will help to supply these data. Also, the kinetics of the chemical species redistribution to the cladding and the chemical states of the fission products will need further investigations.

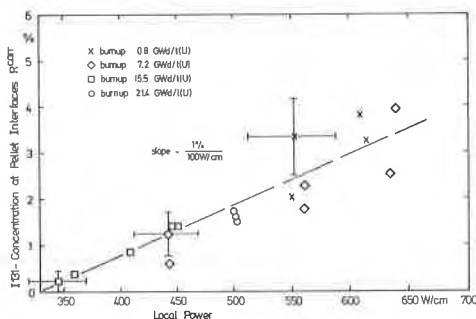


Figure 3 Measured I-131 Concentration at Pellet Interfaces of Rodlets with Different Burnups

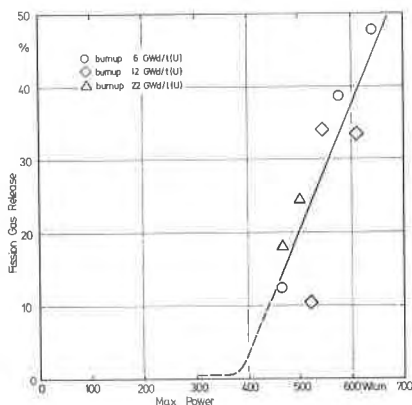


Figure 4 Measured Fission Gas Release of Rodlets with Different Burnups

5. References

- /1/ Holzer, R. and Stehle, H. "Results and Analysis of KWU Power Ramp Investigations", KTG/ENS/JRC Meeting on Ramping and Load-Following Behaviour of Reactor Fuel, Petten, Dec.(1978)
- /2/ Garzarolli, F., Manzel, R., Peehs, M. and Stehle, H. "Observations and Hypothesis on Pellet-Clad Interaction Failures" Kerntechnik, 20, 27 (1978)
- /3/ Vogl, W., Markgraf, J., Ruyter, I. "Stand der Leistungsrampenversuche mit LWR-Brennstäben im HFR Petten" Proc. Dt. Reaktortagung Hannover 1978, 533 (1978)
- /4/ Ruyter, I., Markgraf, J., Vogl, W., "Petten Ramping Experiments with Pre-irradiated Test Fuel rods, Some Preliminary Results", Enlarged Halden Program Group Meeting, Sanderstølen, March (1977)
- /5/ Sontheimer, F., Vogl, W., to be published
- /6/ Peehs, M., Stehle, H. and Steinberg, E. "Out-of-Pile Testing of Iodine Stress Corrosion Cracking in Zircaloy Tubing under the Aspect of the PCI-Phenomenon", ASTM Zirconium Conference, Stratford upon Avon, June (1978)
- /7/ Wunderlich, F., Distler, I., Fuchs, H.P. and Hering, W. "Ein Interferenz-Modell zur Beurteilung des Rampenverhaltens von LWR-Brennstäben", Proc. Dt. Reaktortagung Mannheim 1977, 469 (1977)
- /8/ Thomas, R.G. "The Studsvik Inter-Ramp Project. An International Power Ramp Experimental Program", KTG/ENS/JRC Meeting on Ramping and Load-Following Behaviour of Reactor Fuel, Petten, Dec.(1978)
- /9/ Vogl, W., Gärtner, M., Pott, G., Ruyter, I., "Leistungsrampenversuche IFA 407 zum Betriebsverhalten von LWR-Brennstäben bei schnellen Leistungserhöhungen", Proc. Dt. Reaktortagung Düsseldorf 1976, 454 (1976)

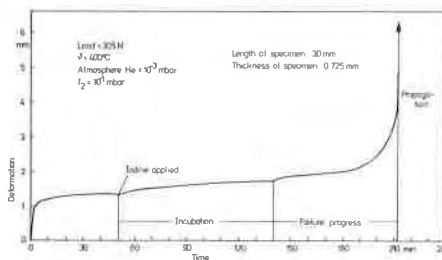


Figure 5 Deformation Behaviour of a Split Ring Specimen in the I-SCC Laboratory Test (Reference /6/)

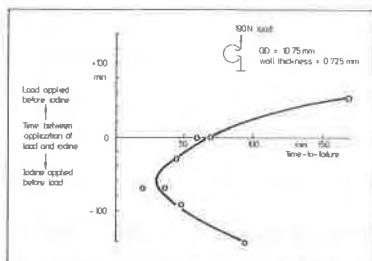


Figure 6 Influence of Load and Iodine Application Times on I-SCC Time to Failure

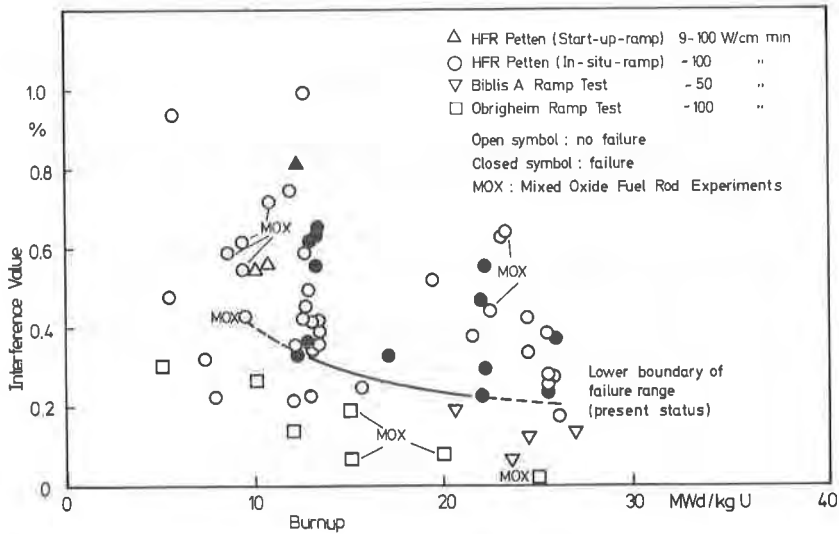


Figure 7 Evaluation of Fast Ramp Tests, Interference Versus Burnup for PWR Fuel Rods (Pre-Pressurized)

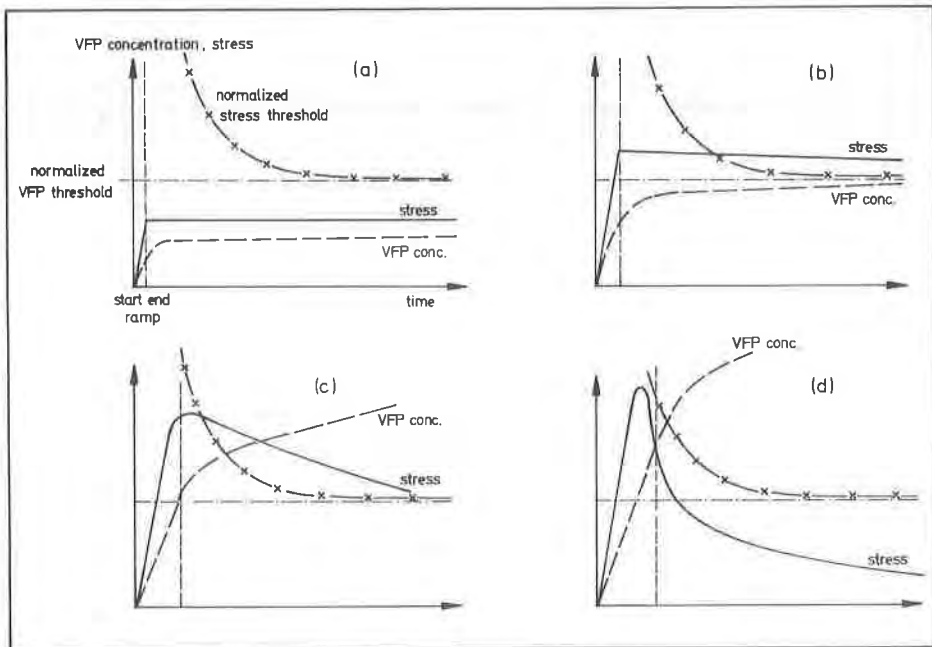


Figure 8 PCI Failure Hypothesis for Fast Ramps with Fixed Ramp Rate

- (a) ramp power below failure threshold
- (b) ramp power at failure threshold
- (c) ramp power in failure region
- (d) ramp power above failure region